Supporting Information

DNA-based digital Comparator System Constructed by Multifunctional Nanoswitches

Hongmei Geng,[ab] Chunyang Zhou,[a]* Chunlei Guo,[ac]*

[a] *The Guo China-US Photonics Laboratory, State Key Laboratory for Applied Optics, Changchun Institute of Optics, Fine Mechanics and Physics, Chinese Academy of Sciences, Changchun, Jilin, 130033, P. R. China.*

[b] *University of Chinese Academy of Sciences, Beijing 100049, China.*

[c] *The Institute of Optics, University of Rochester, Rochester, New York, 14627, USA.*

Email: guo@optics.rochester.edu

Table S1 Sequences of the oligonucleotides used in this work.

Name	DNA Sequence (from 5' terminal to 3' terminal)
P01	FAM- TAAGTCAGTGTGGAACCTTCTGACTTA –Q1
P02	TTTGGGTGGGTGGGTGGGTTAA
P03	Cy5- AACGTCGGATCCCGCAAACAAGCCCGACGTT –Q2
A0	GGTGGGTAATCCCGCGTGCTAGAGATTTTCCACACTGACTTAC TTAAACCCACCCACCC
B0	GGTGGGTTAATGTGGAAAATGGCGACGCGGGATCCGACGTTA CTAAACCCACCCACCC
$P1_{2-3}$	FAM- TTCAATTTAACCAACCTTCCAAATTGAA –Q1
$P2_{2-3}$	TTTGGGTGGGTGGGTGGGTT
$P3_{2-3}$	Q2- CCTTAAACCCTTGGTTTGTTTAAGGA -Cy5
A1	CCTTAAACCCACCCAGGGTTGGTTAAATTGAA
B1	TTCAATTTAACCAACCCACCCAAGGGTTTAAGG
$P1_{3-3}$	Q1- CCTAACAATACTTCACATTAACATTTATTGTTAGGTA -FAM
$P2_{3-3}$	TTTGGGTGGGTGGGTGGGTT
$P3_{3-3}$	Cy5- AACAATAAATATTACACTTCTTACATAATATTGTT -Q2
A2	AATAACCTAACAATA AATGTTAAACCCACCTTTCCACCC
B2	GGGTGGACCTAACAATAAATGTTAAACCCACCTTTCCACCC
C2	GGGTGGATGTAATATTTATTGTTAAACCCACCTTTCCACCC
$P1_{4-3}$	FAM- TTTAACACTTTCTACCTTTGTGTTA AA -Q1
$P2_{4-3}$	ATTGGGTGGGTGGGTGGGTTTAAATC
$P3_{4-3}$	Q2- TAACTATTGACCCACTTAACAATAGTTA -Cy5
A3	TTAAACCCACCCACCCTGGGTTGTAGAAAGTGTTAAACTTAAC AATA
B3	TTTAACACAAAGGTATTCTGGGTGATTTAAACCCACCCACACT TAACAA
C3	AACACTTTCTACATTTAAACCCACCCAGTGGGTCAATAGTTAC TTTGTGT
D3	TAACTATTGTTAAGTGTGGGGAATCTTTAAACCCACCCACCTT TGTGT
HIV-s1	GGTGGGTAATCCCGCGTGCTAGAGATTTTCGACACTGACTTAC TTAAACCCACCCACCC
HIV-s2	GGTGGGTAATCCCGCGTGCTAGAGATTTTCCACACTGTTTTAC TTAAACCCACCCACCC
HIV-s3	GGTGGGTAATCCCGCGTGCTAGAGATTTTGGACACTGACTTAC TTAAACCCACCCACCC
HIV-s4	GGTGGGTAATCCCGCGTGCTAGAGATTTTCCACACTGTAATAC TTAAACCCACCCACCC
HIV-s5	GGTGGGTAATCCCGCGTGCTAGAGATTTGGGACACTGACTTAC TTAAACCCACCCACCC
HCV -	GGTGGGTTAATGTGGAAAATGGCGACGCGAGATCCGACGTTA

s1	CTAAACCCACCCACCC
HCV - s2	GGTGGGTTAATGTGGAAAATGGCGACGCGGGATCCGAGCTTA CTAAACCCACCCACCC
HCV - s3	GGTGGGTTAATGTGGAAAATGGCGACGCAAGATCCGACGTTA CTAAACCCACCCACCC
HCV - s4	GGTGGGTTAATGTGGAAAATGGCGACGCGGGATCCGTGCTTA CTAAACCCACCCACCC
HCV - s5	GGTGGGTTAATGTGGAAAATGGCGACGAAAGATCCGACGTTA CTAAACCCACCCACCC

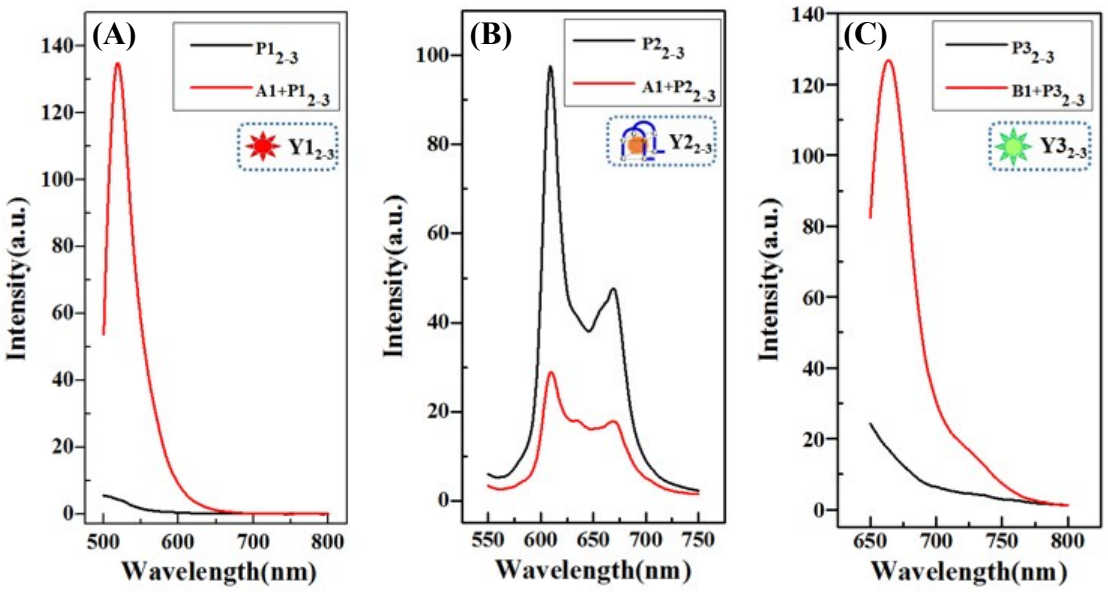

Figure S1. (A) The photographs of $P1_{2\text{-}3}$ before (black curve) and after hybridized with corresponding DNA (red curve). (B) The photographs of $P2_{2\text{-}3}$ before (black curve) and after hybridized with corresponding DNA (red curve). (C) The photographs of $P3_{2\text{-}3}$ before (black curve) and after hybridized with corresponding DNA (red curve).

In order to illustrate how the reaction platform performs the function of signal switch, the dim fluorescences of $P1_{2\text{-}3}$ and $P3_{2\text{-}3}$ and the enhanced fluorescence of $P2_{2\text{-}3}$ was defined as the initial state (Figure S1, black curves). When the $P1_{2\text{-}3}$, $P2_{2\text{-}3}$ and $P3_{2\text{-}3}$ were hybridize with their complementary strands (A1 and B1), the dim fluorescence of $P1_{2\text{-}3}$ and $P3_{2\text{-}3}$ could be lightened up and the enhanced fluorescence of $P2_{2\text{-}3}$ could be quenched (Figure S1A, S1B and S1C, red curves).

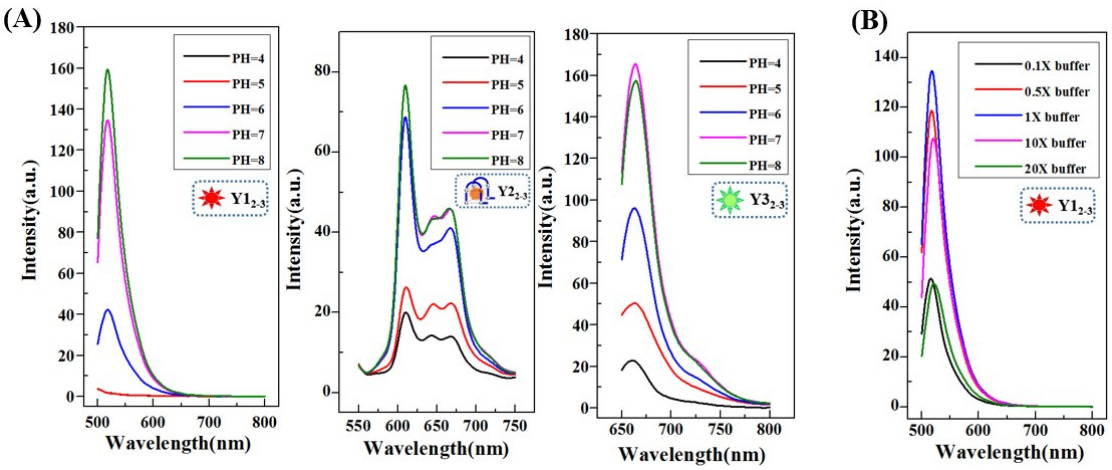

Figure S2. The optimization of the pH value (A) and buffer concentration (B) for the operation of DC logic system.

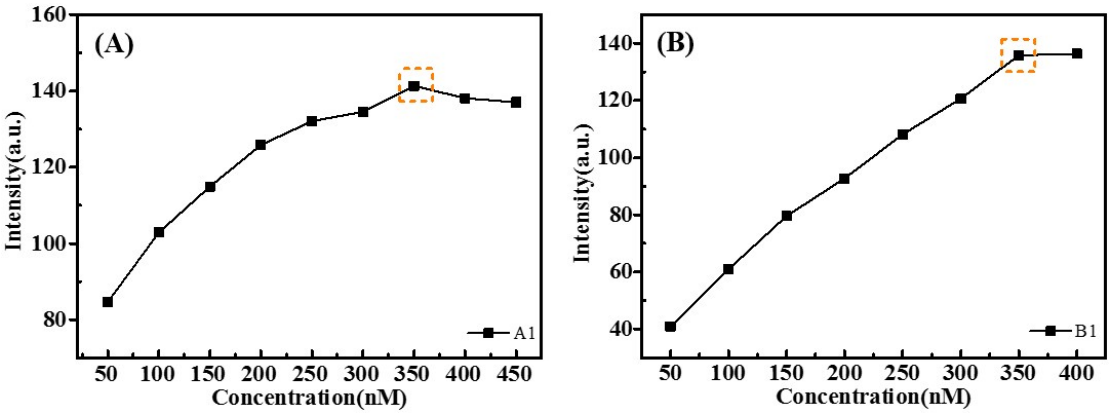

Figure S3. The FAM and Cy5 fluorescence response of $P1_{2\text{-}3}$ and $P3_{2\text{-}3}$ in DNA switch-based platform at 517 and 632 nm with increasing the concentrations of A1 (A) and B1 (B).

Before the operation of 2-3 logic circuit, different concentrations of inputs including A1 and B1 were optimized with DNA switch-based platform (the concentrations of $P1_{2\text{-}3}$, $P2_{2\text{-}3}$ and $P3_{2\text{-}3}$ were all 100 nM) based on the fluorescence of FAM and Cy5 modified on the end of $P1_{2\text{-}3}$ and $P3_{2\text{-}3}$. As shown in Figure S3A, with the increase concentration of A1, the trend of fluorescence intensity reached the maximum at 350 nM and remained basically the same via FRET, showing the optimized concentration of A1 was 350 nM in 2-3 logic operation. As shown in Figure S3B, with the increase concentration of B1, the trend of fluorescence intensity also reached the maximum at 350 nM and remained basically the same, which showed the optimized concentration of B1 was 350 nM.

Input		Output		
A1	B1	$Y1_{2\text{-}3}$	$Y2_{2\text{-}3}$	$Y3_{2\text{-}3}$
0	0	0	1	0
1	0	1	0	0
0	1	0	0	1
1	1	0	1	0

Figure S4. The truth table of 2-3 logic operation.

From the truth table of 2-3 logic operation we can get that, for input signals, the absence of input DNA strands (A1 and B1) were set as "0", otherwise, they were set as "1" for their presence. The $Y1_{2\text{-}3}$ represented the comparison of input signals was A1>B1 (1>0) when the presence of A1. The $Y2_{2\text{-}3}$ represented the comparison of input signals was A1=B1 when the coexistence of A1 and B1 or not (1=1 or 0=0). The $Y3_{2\text{-}3}$ represented the comparison of input signals was A1<B1 (0<1) when the presence of B1.

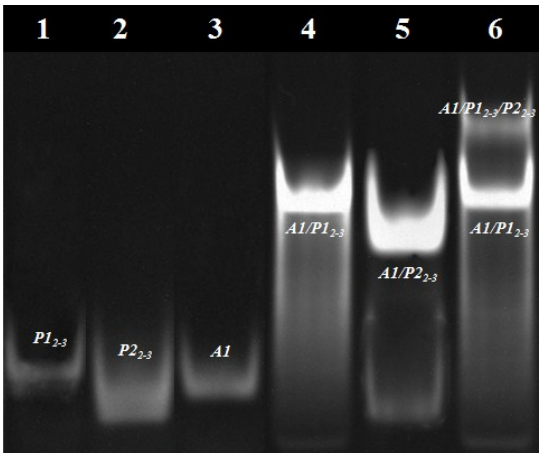

Figure S5. PAGE experiments to further prove the formation of the duplex of A1/P1$_{2-3}$/P2$_{2-3}$. Different DNA samples were added into lanes 1−6. Lane 1: P1$_{2-3}$, Lane 2: P2$_{2-3}$, Lane 3: A1, Lane 4: P1$_{2-3}$+A1, Lane 5: P1$_{2-3}$+A1, Lane 6: P1$_{2-3}$+P1$_{2-3}$+A1.

The PAGE experiments were performed to further identify the hybridization between P1$_{2-3}$, P2$_{2-3}$ and A1. All DNA sequences mentioned in this experiment that contained in different belts have been determined. From Lane 1 to Lane 3, the bands exhibited the single-stranded DNA of P1$_{2-3}$ and P2$_{2-3}$, and A1, which appeared in different positions. When A1 was added to P1$_{2-3}$, the new band formed in Lane 4 represented the formation of duplex of A1/P1$_{2-3}$. With the addition of A1 to P2$_{2-3}$, a new band appeared in Lane 5, indicating the formation of duplex of A1/P2$_{2-3}$. However, when the addition of A1 to the mixture of P1$_{2-3}$ and P2$_{2-3}$, two new bands appeared in Lane 6. The lower one was proved to the duplex of A1/P1$_{2-3}$, which performed the same position compared to the new band appeared in Lane 4. Also, we could conclude that the upper one was proved to the duplex of A1/P1$_{2-3}$/ P2$_{2-3}$ by comparing with Lane 4 and Lane 5. The PAGE results validated the DNA reaction between the P2$_{2-3}$, P2$_{2-3}$, and A1 as expected, which were consistent with the fluorescence results in Figure 1B (line b).

Input			Output		
M		N			
A2	B2	C2	$Y1_{3\text{-}3}$	$Y2_{3\text{-}3}$	$Y3_{3\text{-}3}$
0	0	0	0	1	0
1	0	0	1	0	0
0	1	0	1	0	0
0	0	1	0	0	1
1	1	0	1	0	0
1	0	1	1	0	0
0	1	1	0	1	0
1	1	1	1	0	0

Figure S6. The truth table of 3-3 logic operation.

As shown in the truth table of the 3-3 DC logic circuit, the third input of C2 (also named as N for convenience) was introduced to properly mimic its function of comparing it with A2B2, which combined the inputs of A2 and B2 as a two-bite binary number and named as M for convenience. For input signals, the absence of input DNA strands (A2, B2 and C2) were set as "0", otherwise, they were set as "1" for their presence. This resulting truth table clearly showed the 3-3 DC logic system executed the binary comparison operations of M>N, M=N and M<N (including the comparisons of 00=0, 01=1, 01>0, 10>0, 11>0, 10>1, 11>1 and 00<1) when the $Y1_{3\text{-}3}$, $Y2_{3\text{-}3}$ and $Y3_{3\text{-}3}$ were defined as "1", respectively.

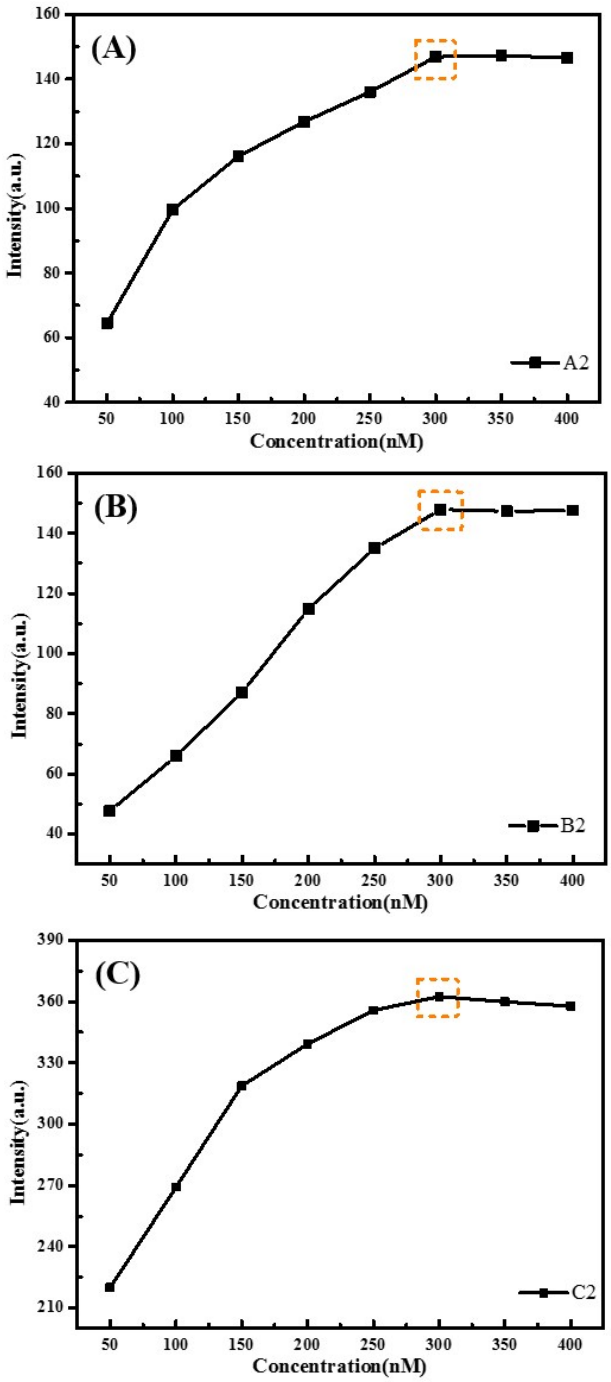

Figure S7. The FAM and Cy5 fluorescence response of $P1_{3\text{-}3}$ and $P3_{3\text{-}3}$ in DNA switch-based platform at 517 and 632 nm with increasing the concentrations of A2 (A), B2 (B) and C2 (C).

Before the operation of 3-3 logic circuit, different concentrations of inputs including A2, B2 and C2 were optimized with DNA switch-based platform (the concentrations of $P1_{3\text{-}3}$, $P2_{3\text{-}3}$ and $P3_{3\text{-}3}$ were all 100 nM) based on the fluorescence of FAM and Cy5

modified on the end of $P1_{3\text{-}3}$ and $P3_{3\text{-}3}$. As shown in Figure S7A, with the increase concentration of A2, the trend of fluorescence intensity reached the maximum at 300 nM and remained basically the same via FRET, showing the optimized concentration of A2 was 300 nM in 3-3 logic operation. As shown in Figure S7B, with the increase concentration of B2, the trend of fluorescence intensity reached the maximum at 300 nM and remained basically the same, which showed the optimized concentration of B2 was 300 nM. As shown in Figure S7C, with the increasing concentration of C2, the trend of fluorescence intensity also reached the maximum at 300 nM and remained basically the same, which showed the optimized concentration of C2 was 300 nM.

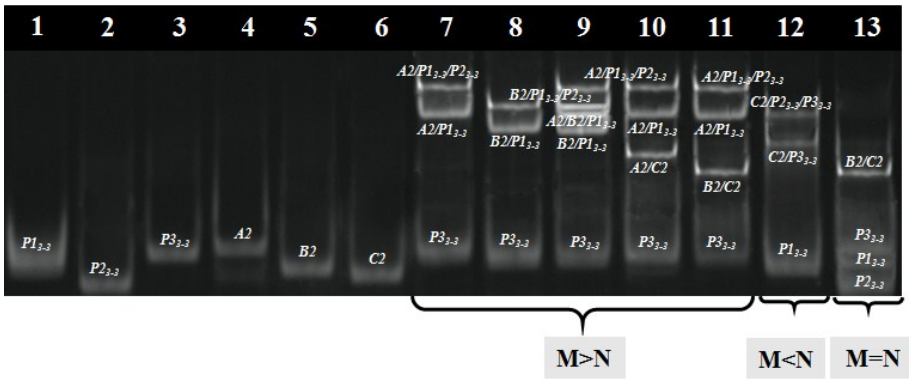

Figure S8. Native polyacrylamide gel (15%) analysis of the interaction among DNA switch-based platform (P, including $P1_{3\text{-}3}$, $P2_{3\text{-}3}$ and $P3_{3\text{-}3}$), A2, B2 and C2 used in the operation of 3-3 DC logic circuit. Lane 1: $P1_{3\text{-}3}$, Lane 2: $P2_{3\text{-}3}$, Lane 3: $P3_{3\text{-}3}$, Lane 4: A2, Lane 5: B2, Lane 6: C2, Lane 7: P+A2, Lane 8: P+B2, Lane 9: P+A2+B2, Lane 10: P+A2+C2, Lane 11: P+A2+B2+C2, Lane 12: P+C2, Lane 13: P+B2+C2.

The PAGE experiments were performed to further identify the hybridization between inputs and platform during the 3-3 DC operations (Figure S8). All DNA sequences mentioned in this 3-3 logic operation that contained in different belts have been determined. From Lane 1 to Lane 6, the bands exhibited the DNA switch of $P1_{3\text{-}3}$, $P2_{3\text{-}3}$, $P3_{3\text{-}3}$, and the individual single-stranded DNA of A2, B2 and C2, which appeared in different positions. Upon the addition of A2 to the DNA switch-based platform, two new bands appeared in Lane 7. The upper one indicated the formation of duplex $A2/P1_{3\text{-}3}/P2_{3\text{-}3}$ and the lower one showed the formation of duplex A2/ $P1_{3\text{-}3}$, leaving $P3_{3\text{-}3}$ in initial position. When the addition of B2 to the platform, two new bands appeared and represented the hybridization of B2 with both $P1_{3\text{-}3}$ and $P2_{3\text{-}3}$ (the upper band) in Lane 8. When the coexistence of A2 and B2 in the platform, they all could hybridize with both $P1_{3\text{-}3}$ and $P2_{3\text{-}3}$ and form the new bands in Lane 9. When A2 and C2 were added to the platform, A2 was designed to hybridize with not only C2 but also the platform of $P1_{3\text{-}3}$ and $P2_{3\text{-}3}$, forming the new bands representing the duplex of $A2/P1_{3\text{-}3}/P2_{3\text{-}3}$ and A2/C2 and leaving the $P3_{3\text{-}3}$ alone in its initial position in Lane 10. When A2, B2 and C2 were all introduced into the platform, B2 had the priority to hybridize with C2 and A2 could hybridize with both $P1_{3\text{-}3}$ and $P2_{3\text{-}3}$, forming the

corresponding bands labeled in Lane 11. When C2 was added to the platform, it could hybridize with both $P2_{3\text{-}3}$ and $P3_{3\text{-}3}$, forming two new bands represented the duplex of C2/ $P2_{3\text{-}3}$ and C2/ $P3_{3\text{-}3}$ in Lane 12. When the addition of B2 and C2 to the platform, they had the priority to hybridize with each other, forming a new band and leaving the platform alone in their positions in Lane 13. The PAGE results validated the DNA reaction of 3-3 DC logic circuit occurred as expected, which were consistent with the fluorescence results in Figure 2B.

	Input				Output		
	X		Y				
	A3	B3	C3	D	$P1_{4-3}$	$P2_{4-3}$	$P3_{4-3}$
1	0	0	0	0	0	1	0
2	1	0	0	0	1	0	0
3	0	1	0	0	1	0	0
4	0	0	1	0	0	0	1
5	0	0	0	1	0	0	1
6	1	1	0	0	1	0	0
7	1	0	1	0	0	1	0
8	1	0	0	1	1	0	0
9	0	1	1	0	0	0	1
10	0	1	0	1	0	1	0
11	0	0	1	1	0	0	1
12	1	1	1	0	1	0	0
13	1	1	0	1	1	0	0
14	1	0	1	1	0	0	1
15	0	1	1	1	0	0	1
16	1	1	1	1	0	1	0

Figure S9. The truth table of the 4-3 logic operation.

The corresponding truth table showed the 4-3 DC logic system executed the binary comparison operations of X>Y, X=Y and X<Y, in which X represented the combination of the inputs of A3 and B3 as a two-bite binary number and Y represented the combination of C3 and D3 as a two-bite binary number for convenience. For input signals, the absence of input DNA strands (A3, B3, C3 and D3) were set as "0", otherwise, they were set as "1" for their presence. This resulting truth table clearly showed the binary comparison operations of 10>00, 01>00, 11>00, 10>01, 11>10, 11>01 when the $Y1_{4-3}$ was defined as "1", 00=00, 10=10, 01=01, 11=11 when the $Y2_{4-3}$ was defined as "1" and 00<10, 00<01, 00<11, 01<10, 10<11, 01<11 when the $Y3_{4-3}$ was defined as "1".

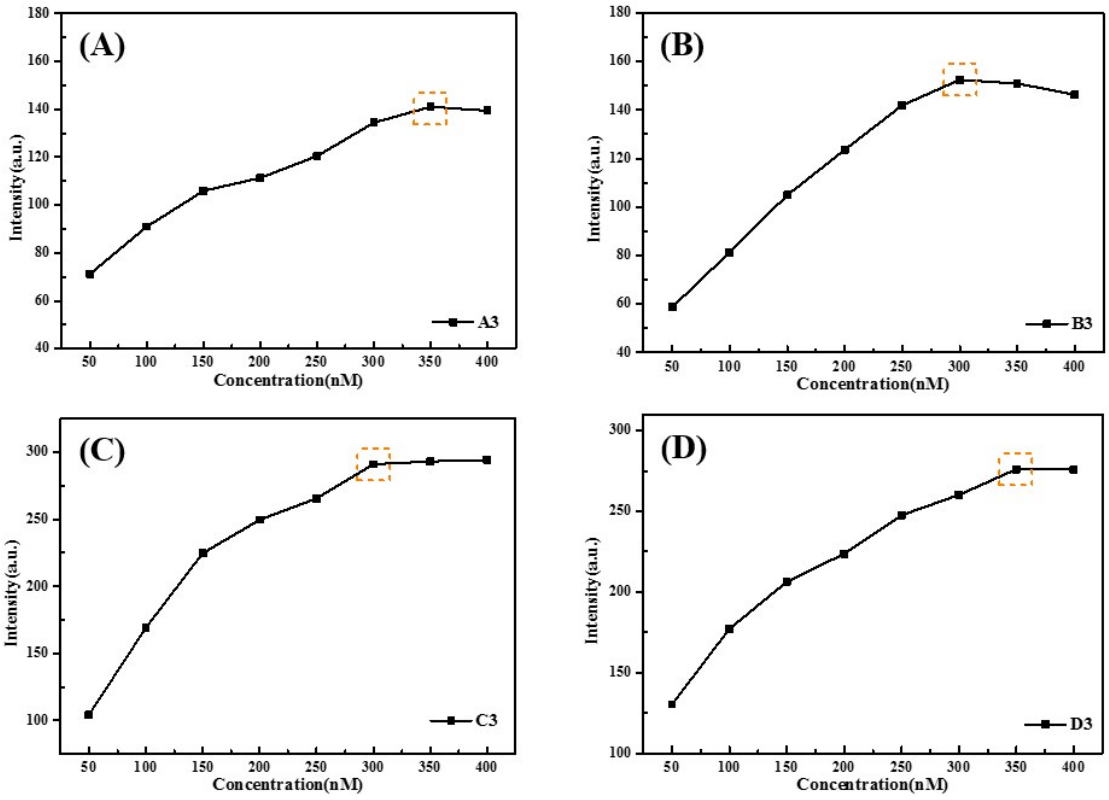

Figure S10. The FAM and Cy5 fluorescence response of $P1_{4\text{-}3}$ and $P3_{4\text{-}3}$ in DNA switch-based platform at 517 and 632 nm with increasing the concentrations of A3 (A), B3 (B), C3 (C) and D3 (D).

Before the operation of 4-3 logic circuit, different concentrations of inputs including A3, B3, C3 and D3 were optimized with DNA switch-based platform (the concentrations of $P1_{4\text{-}3}$, $P2_{4\text{-}3}$ and $P3_{4\text{-}3}$ were all 100 nM) based on the fluorescence of FAM and Cy5 modified on the end of $P1_{4\text{-}3}$ and $P3_{4\text{-}3}$. As shown in Figure S10A, with the increase concentration of A3, the trend of fluorescence intensity reached the maximum at 350 nM and remained basically the same via FRET, showing the optimized concentration of A3 was 350 nM in 4-3 logic operation. As shown in Figure S10B, with the increase concentration of B3, the trend of fluorescence intensity reached the maximum at 300 nM and remained basically the same, which showed the optimized concentration of B3 was 300 nM. As shown in Figure S10C, with the increase concentration of C3, the trend of fluorescence intensity also reached the maximum at 300 nM and remained basically unchanged, which showed the

optimized concentration of C3 was 300 nM. As shown in Figure S10D, with the increase concentration of D3, the trend of fluorescence intensity reached the maximum at 350 nM and remained basically unchanged, which showed the optimized concentration of D3 was 350 nM.

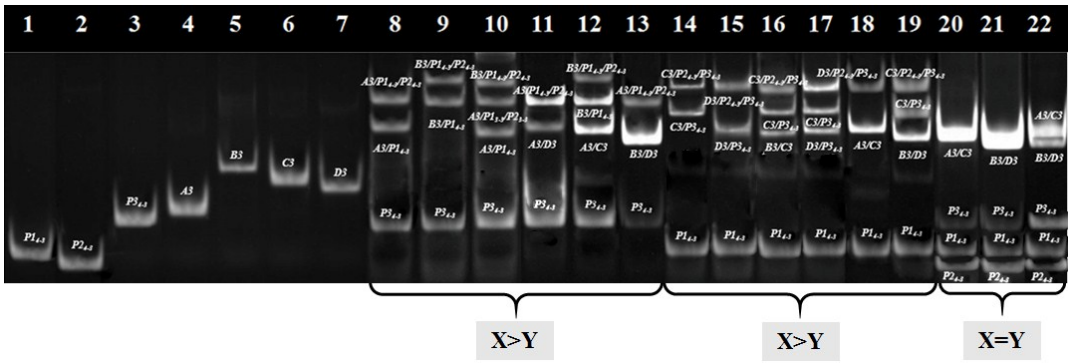

Figure S11. Native polyacrylamide gel (15%) analysis of the interaction among DNA switch-based platform (P, including $P1_{4-3}$, $P2_{4-3}$ and $P3_{4-3}$), A3, B3, C3 and D3 used in the operation of 4-3 DC logic circuit. Lane 1: $P1_{4-3}$, Lane 2: $P2_{4-3}$, Lane 3: $P3_{4-3}$, Lane 4: A3, Lane 5: B3, Lane 6: C3, Lane 7: D3, Lane 8: P+A3, Lane 9: P+B3, Lane 10: P+A3+B3, Lane 11: P+A3+D3, Lane 12: P+A3+B3+C3, Lane 13: P+A3+B3+D3, Lane 14: P+C3, Lane 15: P+D3, Lane 16: P+B3+C3, Lane 17: P+C3+D3, Lane 18: P+A3+C3+D3, Lane 19: P+B3+C3+D3, Lane 20: P+A3+C3, Lane 21: P+B3+D3, Lane 22: P+A3+B3+C3+D3.

The PAGE experiments were performed to further identify the hybridization between inputs and platform during the 4-3 DC operations. All DNA sequences mentioned in this 4-3 logic operation that contained in different belts have been determined. From Lane 1 to Lane 7, the bands exhibited the DNA switch of $P1_{4-3}$, $P2_{4-3}$, $P3_{4-3}$, and the individual single-stranded DNA of A3, B3, C3 and D3, which appeared in different positions. In the case of X>Y, when the addition of A3 to the DNA switch-based platform, two new bands appeared in Lane 8. The upper one indicated the formation of duplex A3/$P1_{4-3}$/$P2_{4-3}$ and the lower one showed the formation of duplex A3/$P1_{4-3}$. When the addition of B3 to the platform, two new bands appeared in Lane 9, indicating the formation of duplex B3/$P1_{4-3}$/$P2_{4-3}$. Similar to the reaction mechanism described above, the coexistence of A3 and B3 performed the same hybridization shown in Lane 10. When the addition of A3 and D3 to the platform, A3 was designed to hybridize with not only D3 but also the platform of $P1_{4-3}$ and $P2_{4-3}$, forming the new bands representing the duplex of A3/$P1_{4-3}$/$P2_{4-3}$ in Lane 11. When A3, B3 and C3

were introduced into the platform, A3 had the priority to hybridize with C3 and B3 could hybridize with both $P1_{4\text{-}3}$ and $P2_{4\text{-}3}$, forming the corresponding bands of the duplex of A3/C3 and B3/$P1_{4\text{-}3}$/$P2_{4\text{-}3}$ in Lane 12. When A3, B3 and D3 were introduced into the platform, B3 had the priority to hybridize with D3 and A3 could hybridize with both $P1_{4\text{-}3}$ and $P2_{4\text{-}3}$, forming the corresponding bands of the duplex of B3/D3 and A3/$P1_{4\text{-}3}$/$P2_{4\text{-}3}$ in Lane 13. Furthermore, $P3_{4\text{-}3}$ had no reaction with the inputs and stayed in its initial position in the case of X>Y. In the case of X<Y, when C3 or D3 was added to the platform, each of them could hybridize with both $P2_{4\text{-}3}$ and $P3_{4\text{-}3}$, forming the new bands represented the duplex of C3/$P1_{4\text{-}3}$/$P2_{4\text{-}3}$ and D3/$P1_{4\text{-}3}$/$P2_{4\text{-}3}$ shown in Lane 14 and Lane 15. Similar to the reaction mechanism described above, the coexistence of C3 and D3 performed the same hybridization shown in Lane 17. When the addition of B3 and C3 to the platform, C3 was designed to hybridize with not only B3 but also the platform of $P2_{4\text{-}3}$ and $P3_{4\text{-}3}$, forming the new bands representing the duplex of C3/$P1_{4\text{-}3}$/$P2_{4\text{-}3}$ in Lane 16. When A3, C3 and D3 were introduced into the platform, C3 had the priority to hybridize with A3 and D3 could hybridize with both $P2_{4\text{-}3}$ and $P3_{4\text{-}3}$, forming the corresponding bands of the duplex of A3/C3 and D3/$P1_{4\text{-}3}$/$P2_{4\text{-}3}$ in Lane 18. When the addition of B3, C3 and D3 to the platform, D3 had the priority to hybridize with B3 and C3 could hybridize with both $P2_{4\text{-}3}$ and $P3_{4\text{-}3}$, forming the corresponding bands of the duplex of B3/D3 and C3/$P1_{4\text{-}3}$/$P2_{4\text{-}3}$ in Lane 19. Also, $P1_{4\text{-}3}$ had no reaction with the inputs and stayed in its initial position when X<Y. In the case of X=Y, upon the addition of A3 and C3 to the DNA switch-based platform, they preferred to hybridize together while they did not hybridize with the DNA-based switches, forming the new band of the duplex of A3/C3 in Lane 20. When the coexistence of B3 and D3, they also preferred to hybridize together and formed the new band of the duplex of B3/D3 in Lane 21. Similar to the reaction mechanism described above, the coexistence of A3, B3, C3 and D3 performed the same hybridization shown in Lane 22. In this case of X=Y, the DNA strands, $P1_{4\text{-}3}$, $P2_{4\text{-}3}$ and $P3_{4\text{-}3}$ in the platform, didn't hybridize with the inputs and were in their initial positions. The PAGE results validated the DNA reaction of 4-3 DC logic circuit occurred as expected, which were consistent with the fluorescence

results in Figure 3B.

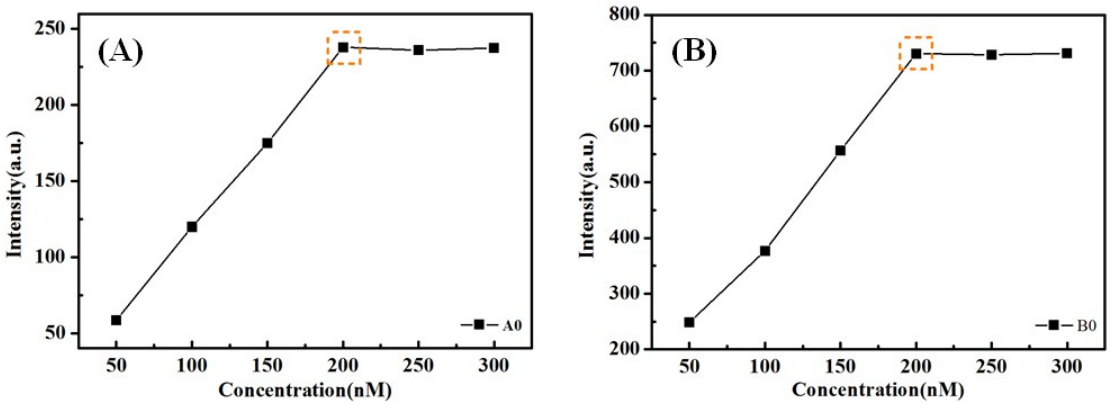

Figure S10. The FAM and Cy5 fluorescence response of P01 and P03 in DNA switch-based platform at 517 and 632 nm with increasing the concentrations of A0 (A) and B0 (B).

Before the operation of mismatched experiments, different concentrations of inputs including A0 and B0 were optimized with DNA switch-based platform (the concentrations of P01, P02 and P03 were all 200 nM) based on the fluorescence of FAM and Cy5 modified on the end of P01 and P03. As shown in Figure S12A, with the increase concentration of A0, the trend of fluorescence intensity reached the maximum at 200 nM and remained basically the same via FRET, showing the optimized concentration of A0 was 200 nM in selectivity operation. As shown in Figure S12B, with the increase concentration of B0, the trend of fluorescence intensity reached the maximum at 200 nM and remained basically the same, which showed the optimized concentration of B0 was 200 nM.

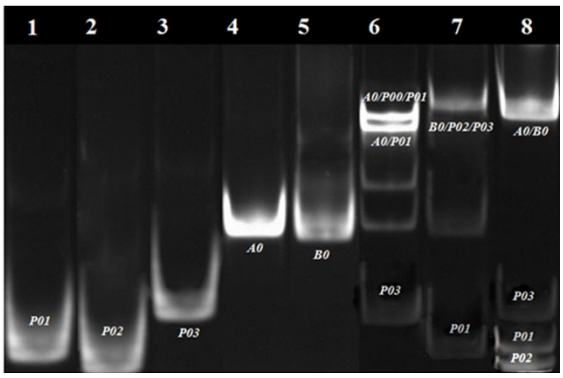

Figure S13. Native polyacrylamide gel (15%) analysis of the interaction among the 2-3 DC-based biosensing system. Different DNA samples were added into lanes 1−8. Lane 1: P01, Lane 2: P02, Lane 3: P03, Lane 4: A0, Lane 5: B0, Lane 6: P01+P02+P03+A0, Lane 7: P01+P02+P03+B0, Lane 8: P01+P02+P03+A0+B0.

The PAGE experiments were performed to further identify the hybridization between inputs and platform during the 2-3 DC-based biosensing system. All DNA sequences mentioned in this system that contained in different belts have been determined. From Lane 1 to Lane 5, the bands exhibited the DNA biosensing of P01, P02, P03, and the individual single-stranded DNA of A0 and B0, which appeared in different positions. When the addition of A0 to the DNA biosensing platform, two new bands appeared in Lane 6. The upper one indicated the duplex of A0/P01/P02 and the lower one showed the duplex of A0/P01. Further, the lowest band illustrated that the P03 didn't react with A0 and stayed in initial position. When the addition of B0 to the platform, two new bands appeared in Lane 7, indicating the formation of duplex of B0/P02/P03 and leaving the P01 in its initial position. When the coexistence of A0 and B0, they hybridized preferentially and formed a new band of the duplex of A0/B0 in Lane 8. Therefore, the DNA strands, P01, P02 and P03 in the platform, didn't hybridize with the inputs, staying their initial positions. The PAGE results validated the DNA reaction of biosensing system occurred as expected, which were consistent with the fluorescence results in Figure 5B.